https://doi.org/10.5194/egusphere-2024-3781
Preprint. Discussion started: 21 January 2025

Numerical quantitation on the effect of coating materials on the mixing state retrieval accuracy of fractal black carbon based on single particle soot photometer

Jia Liu[1, 2, 3], Donghui Zhou[2, 3], Guangya Wang[2, 3], Cancan Zhu[2, 3], and Xuehai Zhang[4]

[1]Department of Atmospheric and Oceanic Sciences and Institutes of Atmospheric Sciences, Fudan University, Shanghai 200438, China.
[2]Engineering Research Center of Zero-carbon Energy Buildings and Measurement Techniques, Ministry of Education, Hebei University, Baoding 071002, China.
[3]China Meteorological Administration Xiong'an Atmospheric Boundary Layer Key Laboratory, Baoding 071800, China.
[4]School of Information Science and Engineering, Henan University of Technology, Zhengzhou 450001, China.

Correspondence: Jia Liu (liujia@hbu.edu.cn)

Abstract. Atmospheric black carbon (BC) particles have complex mixing states, the characterization of BC mixing state is essential for assessment of the radiative effects. The single particle soot photometer (SP2) measures BC mixing state with the coating refractive index is assumed to be constant 1.50+0*i*, which is obviously not suitable for realistic various coating components. In this study, sulfate, non-absorbing organic carbon (OC), and brown carbon (BrC) are selected as typical coatings to numerically quantify the effects of coating material and morphology structure on the retrieval accuracy of BC mixing state. The numerical simulations of BC with thin and thick coatings are conducted using multiple-sphere T-matrix (MSTM), and the mixing state retrievals are based on Mie theory according to the principle of SP2. Results showed that the relative errors of retrieved mixing states for BC coated by sulfate and OC are larger than these for BC coated by BrC, however, the SP2 missed evidently more results of mixing states of BC aerosols coated by BrC. When the retrieved mixing states are employed to assess the absorption enhancement (E_{ab}) and the radiative forcing, BrC coating also leads to larger deviations in E_{ab} than sulfate and OC, the estimation error of radiative forcing of BrC coated BC at 1064 nm wavelength reaches -89.9%, while the corresponding errors for sulfate and OC coatings range from -64.3% to -38.4%. This study highlights the coating materials of BC should be considered when monitoring the mixing state using SP2.

1. Introduction

Black carbon (BC) is an important component of atmospheric aerosol, which is mainly generated from the incomplete combustion of carbon-rich materials such as fossil and biomass (Bond et al., 2013). The sources of BC aerosols can be categorized into two types, one is the violent emission through natural phenomena like forest fires and volcanic eruptions (Murphy et al., 2014; Santoso et al., 2020), and the other is the widespread and persistent anthropogenic emission, which has more contributions to the long-term variations in atmospheric BC concentrations (Zhang et al., 2020). Although BC accounts for a small proportion of atmospheric aerosol, as an absorptive aerosol it strongly absorbs sunlight from the visible to infrared wavelengths, which increases the amount of solar radiation absorbed by the ground-air system and produces a strong positive forcing on climate change (Li et al., 2019). In addition, BC also acts as cloud condensation nuclei, accelerates the melting of snow and ice, alters the atmosphere temperature structure and vertical diffusion of pollutants (Ding et al., 2016; Wang et al., 2015). BC is usually emitted into the atmosphere as primary particulate matter, fresh BC particles usually present as loose chain-like aggregates consisting of a large number of nearly spherical monomers (Ceolato et al., 2020). During transportation and aging in the atmosphere, different chemical components such as organic matter, sulfates, and nitrates condense and coagulate on the surface of BC, the loose aggregates gradually evaluate to dense spherical shapes with complex mixing structures (China et al., 2013; Lei et al., 2020)

The mixing state is a key microphysical property to evaluate the optical and radiative effects of BC aerosols, many instruments have been applied to measure the BC mixing state based on different principles and techniques. Transmission electron microscope (TEM) is a basic instrument for direct off-line observation of BC mixing states through component identification and morphology analysis. The sampling and characterization of atmospheric aerosol in single particle level reveals that the aging of BC aerosol results in structure compactness and coating layers, the morphology and mixing state of BC show enormous diversity (Li et al., 2023; Liu et al., 2020; Wang et al., 2017). Adachi et al. (2014) conducted TEM analyses of aerosol particles with aerodynamic diameters ranging in 60-350 nm, about 10% of collected particles are BC and about 75% of BC particles are mixed with sulfate or other substances. The single particle soot photometer (SP2) can measure the mass and diameter refractory BC (D_c), the optical diameter (D_p), and therefore the mixing state (D_p/D_c) in a single particle level. As an effective online instrument, the SP2 has been widely applied for the measurement of BC mixing states whether be used alone or in tandem with other apparatus to form observation systems (Liu et al., 2020; Liu et al., 2022).

The optical cavity of SP2 is mainly consists of a laser with a wavelength of 1064 nm and four symmetrically arranged detectors covering viewing angles of 13-77° and 103-167° relative to the laser (Gao et al., 2007). When exposed to laser persistently, the bare BC would emit incandescent light, which can be monitored by two detectors, and the peak of incandescent signal is proportional to the mass of BC (Schwarz et al., 2006). Then, the mass and volume equivalent diameter of BC (D_c) can be obtained with its density is set to 1.8 g/cm^3 (Bond and Bergstrom, 2006). As coated BC passes through laser beam vertically, the coating would be heated and evaporate, thus the scattered light recorded by the other two detectors is dynamically evolved. The leading edge of original scattered light signal when the coated BC entering the light beam is extracted to reconstruct the complete Gaussian scattering signal with the insistence of Leading Edge Only (LEO) method and the position-sensitive detector (Gao et al., 2007). The differential scattering cross-section is derived subsequently, and the optical diameter (D_p) of coated BC can be retrieved based on Mie scattering theory in combination with core-shell model. Finally, the mixing state of coated BC is measured and expressed as D_p/D_c. Furthermore, through the statistical analyses of the lag time between the appearance of scattering signal and incandescent signal, the particles can be classified into thinly coated BC and heavily coated BC.

https://doi.org/10.5194/egusphere-2024-3781
Preprint. Discussion started: 21 January 2025

Measurement errors in BC core size and differential scattering property of coated BC using SP2 can be calibrated regularly through Aquadag soot and polystyrene particles. However, since the morphologies and coating structures of aged BC aerosol are complicated, thus the optical retrieval of mixing states of BC would introduce evident errors due to the oversimplification of particle model. Firstly, both the BC core and the coating are assumed to be spherical and forming core-shell structures. In contrast, realistic BC particles can be film-wrapped or encapsulated by coatings, then this significant inconsistency result in errors in optically retrieved equivalent diameter of coated BC (D_p). Our previous studies have explored the effects of fractal morphology and coating structure on the optically retrieved particle size and mixing state of aged BC aerosol, the non-spherical shape of realistic BC bring large retrieval errors in diameter and D_p/D_c, and it is worth noting that optical retrieval based on Mie theory would miss microphysical parameters for a large amount of BC particles (Liu et al., 2023b; Liu et al., 2023c). Besides, the coatings of atmospheric BC aerosols can be inorganic salt like sulfate and organics with absorptive or non-absorptive properties, their refractive indices are not exactly the same, which further affect the optical properties of coated BC. Zhang et al. (2021) investigated the absorption property of BC coated by brown carbon, results showed that the blocking effect on the light absorption enhancement of partially coated BC increases with the increase of coating absorption fraction. However, the current optical retrieval method of SP2 roughly assume the refractive index of all coatings is constant 1.50+0*i*. What and how does this uniform assumption of refractive index affect the retrieved mixing state of BC is indistinct and needs to be quantified.

To answer above questions, in this study, the coupling effects of coating materials and complex morphology on the optical retrieval accuracy of BC mixing states based on Mie theory using SP2 are investigated from the perspective of numerical simulation. State-of-art closed-cell model (CCM) and coated-aggregate model (CAM) are constructed to simulate typical thinly and heavily coated BC which can be classified by lag time. Different aerosol components with their corresponding refractive indices are selected as coatings, and the numerical simulation results of complex models are regarded as realistic optical properties of BC. Referring to the retrieval methodology of SP2, the optical equivalent diameter and mixing state of coated BC are obtained using differential scattering parameters, based on Mie theory and simple core-shell model. Then, the retrieved results of D_p/D_c are compared with the preset values, and the effects of coating materials and coating structures on the BC mixing state retrieval accuracies are quantified. Furthermore, in order to promote the reasonable use of measured D_p/D_c, the prediction performances for essential parameters absorption enhancement (E_{ab}) and radiative forcing (RF) of BC using SP2 measurements are evaluated.

2. Methodology

2.1 Morphological models of BC aerosols

According to the observations using electron microscopes, the morphologies of newly emitted BC particle are not spherical but fractal, a large number of near-spherical monomers clustered together and form a single BC particle. The geometry of bare BC follows the scaling rule:

https://doi.org/10.5194/egusphere-2024-3781
Preprint. Discussion started: 21 January 2025

$$N_s = k_f \left(\frac{R_g}{a_0} \right)^{D_f}, \tag{1}$$

$$R_g = \sqrt{\frac{1}{N_s} \sum_{i=1}^{N_s} r_i^2}, \tag{2}$$

where a_0 is monomer radius, N_s is monomer number, k_f and D_f are pre-factor and fractal dimension controlling the morphology of BC aggregate, R_g is rotation radius that describes spatial scale of BC, and r_i is the distance between the i monomer and mass center of whole aggregate (Kahnert and Kanngiesser, 2020; Zeng et al., 2019). The newly discharged BC particles show loose chain structures with the values of D_f are about 1.80, during the atmospheric aging process, the fractal structure becomes more compact and closes to sphere with D_f increase to about 2.80 and even larger. The pre-factor is assumed to be 1.20, and the monomer radius of BC is fixed to 20 nm, which is a typical value observed in experiments (Li et al., 2003; Sorensen and Roberts, 1997). To cover the most of the size of atmospheric BC, the monomer number ranges from 50 to 2000 with a step of 50, and the volume equivalent diameter of BC core (D_c) can be obtained:

$$D_c = 2a_0 \sqrt[3]{N_s}, \tag{3}$$

Furthermore, the non-BC component tends to cover the surface of BC through aging process, forming complicated film-coated and encapsulated mixing structures. The typical coating species can be light absorptive brown carbon (BrC) and non-absorptive material like organic matter and inorganic salt (Kholghy et al., 2013). For the sake of adequately simulate the complicated non-spherical mixing structure of aged BC with thin or heavy coatings, which is in line with the rough classify method adopt by SP2, two advanced morphological models closed-cell model (CCM) and coated-aggregate model (CAM) are constructed. The CCM with D_f=1.80, 2.20, and 2.60 are employed to represent BC with thin film coatings, while the CAM with D_f=2.60 and 2.80 are employed to represent BC encapsulated by coatings. The amount or volume of coatings are also essential parameters controlling the overall morphology of coated BC, which can be expressed by the volume fraction (V_f) of BC core and the mixing state (D_p/D_c):

$$V_f = \frac{V_{BC}}{V_{total}}, \tag{4}$$

$$\frac{D_p}{D_c} = \frac{1}{\sqrt[3]{V_f}}, \tag{5}$$

where V_{BC} and V_{total} are the volumes of BC core and coated BC respectively, D_p and D_c are the diameters of volume equivalent spheres for coated BC and BC core respectively. The Diffusion-limited aggregation (DLA) algorithm developed

https://doi.org/10.5194/egusphere-2024-3781
Preprint. Discussion started: 21 January 2025

by Wozniak et al. (2012) was employed to generate fractal aggregates firstly. For the construction of the closed-cell model, the original fractal aggregate was enlarged according the BC volume fraction, and a soot sphere was added into each enlarged monomer. As for the coated aggregate model, the fractal aggregate was encapsulated by one single spherical coating (Liu et al., 2023a).

2.2 Numerical simulation of optical properties

In this study, the wavelength of the optical properties simulated is set to 1064 nm, the same wavelength as the laser used in SP2, assuming that the complex refractive index of the BC core and the coating is also the same as the SP2 set values of 2.26-1.26i and 1.50+0i, respectively. The density of the BC core (ρ_{BC}) and the coating ($\rho_{coating}$) is set to 1.80 g/cm^3 and 1.20 g/cm^3(Liu et al., 2014; Zhang et al., 2019). In the error analysis of SP2 measurement of the mixing state of BC by different coating materials, the density of sulfate, non-absorbable organic carbon (OC) and brown carbon (BrC) were set as 1.769 g/cm^3, 1.2 g/cm^3, and 1.2 g/cm^3(Wang et al., 2021; Luo et al., 2021), and the corresponding complex refractive index was set as 1.51+10-5i, 1.52+0.02i, 1.55+0.18i, respectively. In addition, the complex refractive index and density selection of MSTM calculation and Mie scattering calculation are consistent. SP2 can determine the quality of the rBC core according to the detected peak of the incandescent light signal, and then deduce the diameter (D_c) of the BC core according to the set density.

Based on the retrieve principle of SP2 and the differential scattering cross-section of fractal BC particles as a reference, the retrieval of the mixing state (D_p/D_c) is the key to this study. First, the MSTM algorithm is used to calculate the differential scattering cross-section of the BC fractal model with preset volume equivalent particle size ratio ($D_{p,v}/D_{c,v}$) at 1064 nm wavelength. Secondly, the differential scattering cross-section of the core-shell model is calculated using the Mie scattering theory. Finally, by fixing the D_c value of the core-shell model and the $D_{c,v}$ value of the BC fractal model is the same, the D_p value of the core-shell model is changed to retrieve the core-shell model corresponding to the differential scattering cross-section of the core-shell model and the fractal model, and its D_p/D_c is regarded as the retrieve mixing state of the coated particles. Therefore, a search method based on the ordinary least square method is defined in this study. The formula is as follows:

$$\chi^2 = \left[\frac{dC_{sca-MSTM}\left(D_{p,v}\right) - d\,C_{sca-Mie}\left(D_{c,v}\right)}{d\,C_{sca-MSTM}\left(D_{p,v}\right)} \right]^2, \tag{6}$$

where $dC_{sca\text{-}MSTM}$ and $dC_{sca\text{-}Mie}$ are the differential scattering cross sections of the BC fractal model and core-shell model respectively. In addition, the relative error (RE) is used to represent the retrieval error of the BC mixing state:

$$RE = \frac{D_p/D_c - D_{p,v}/D_{c,v}}{D_{p,v}/D_{c,v}} \times 100\%, \tag{7}$$

https://doi.org/10.5194/egusphere-2024-3781
Preprint. Discussion started: 21 January 2025

The microphysical properties of BC aerosols have a significant influence on their optical properties, which in turn affect the radiation effects of BC aerosols. SP2 retrieves the mixing state of BC aerosol based on Mie scattering theory and assumes that BC particles have a spherical core-shell structure. However, the core-shell model is seriously inconsistent with the actual morphology of BC aerosol, so there are inevitable errors in the mixing state obtained by retrieval, which further affects the estimation of the radiation effect of BC aerosol. In this study, the simple forcing efficiency (SFE) equation proposed by Bond and Bergstrom (2006) is used to quantify the radiative forcing estimation error caused by the SP2 mixing state retrieval error. The simple forcing efficiency equation is defined as the radiative forcing normalized by the mass of BC, representing the amount of energy added to the Earth's atmospheric system by particles of a given mass in the atmosphere:

$$MAC = \frac{C_{sca}}{m_{BC}}, \quad (8)$$

$$MSC = \frac{C_{abs}}{m_{total}}, \quad (9)$$

$$m_{BC} = \rho_{BC} V_{BC}, \quad (10)$$

$$m_{total} = \rho_{BC} V_{BC} + \rho_{coating} V_{coating}, \quad (11)$$

$$V_{coating} = \left(1 - V_f\right) V_{BC} / V_f, \quad (12)$$

$$\frac{dSFE}{d\lambda} = -\frac{1}{4}\frac{dS(\lambda)}{d\lambda}\tau^2 \left(1 - F_c\right)\left[2\left(1 - a_s\right)^2 \beta(\lambda) \times MSC(\lambda) - 4 a_s MAC(\lambda)\right], \quad (13)$$

where m_{BC} and m_{total} are the mass of the BC core and the whole BC particle respectively, ρ_{BC} and $\rho_{coating}$ are the density of BC core and coating respectively, and $V_{coating}$ is the volume of coating. According to ASTM G173-03, the atmospheric transmittance τ=0.79, the cloud fraction F_c=0.6, the typical urban surface albedo a_s=0.19, and the backscattering fraction β=0.15.

The absorption enhancement is determined by the ratio of the absorption cross-section of the whole BC particle ($C_{abs,p}$) to that of the bare black carbon core ($C_{abs,c}$), and the specific solution process is shown below:

$$E_{ab} = \frac{C_{abs,p}}{C_{abs,c}}, \quad (14)$$

https://doi.org/10.5194/egusphere-2024-3781
Preprint. Discussion started: 21 January 2025

$$C_{abs,p} = Q_{abs,p} \cdot \pi \left(\frac{D_{p,v}}{2} \right)^2 , \tag{15}$$

$$C_{abs,c} = Q_{abs,c} \cdot \pi \left(\frac{D_{c,v}}{2} \right)^2 , \tag{16}$$

where Qabs,p and Qabs,c are the absorption efficiency of the whole BC particle and the absorption efficiency of the bare BC core respectively, and the corresponding values can be obtained by the MSTM algorithm.

3. Result and discussion

The accuracy of the single-particle soot photometer in retrieving the mixing state of the coated BC particles is not only affected by the structure of the coated BC but also by the composition of the coated BC. Different coating materials have different complex refractive indices, which will affect the optical properties of aerosol particles, and then affect the retrieval of its mixing state. Based on the optical equivalent particle size retrieval principle of SP2, the optical equivalent particle size of the BC in the fractal particle model is taken as the BC core in the core-shell model. Based on Mie scattering, the optical equivalent particle size of the optical equivalent double-layer sphere is obtained. In this chapter, the mixing state of coated BC particles with different coating materials is retrieved. The influence of different coatings materials on the BC mixing state of SP2 retrieval is investigated, and the influence of retrieval errors (RRs) on the estimation of black carbon absorption enhancement and radiative forcing is studied.

3.1 Influence of different coating materials on the retrieval of mixing state

The BC aerosol discharged into the atmosphere makes it very easy to adsorb other aerosols (sulfate, OC, BrC, etc.) to form a mixing state. The difference in microphysical properties of coating materials leads to the difference in their optical properties. The complex refraction index is one of the important factors that determine the microphysical properties of aerosols. The real part of the complex refractive index reflects the scattering ability of aerosols, while the imaginary part reflects the absorption ability of aerosols. According to the set microphysical parameters, the optical property results were obtained through optical calculation, to retrieve the mixing state of BC particles in a real atmospheric environment and explore the influence of different coating materials on the accuracy of measuring BC mixing state with SP2. In order to ensure the maximum amount of data in the retrieval results, the mixing states of BC coated by sulfate, OC, and BrC were respectively retrieved according to the forward scattering. Meanwhile, for different coating materials, two models, closed-cell and coated-aggregate, are also considered to retrieve the actual mixing state of light and heavily coated BC particles.

Figure 1. shows the retrieval results of BC particles coated by sulfates in different typing models. The RE of lightly coated BC particles represented by the closed-cell model coated by sulfate is greater than that of heavily coated BC particles

https://doi.org/10.5194/egusphere-2024-3781
Preprint. Discussion started: 21 January 2025

represented by the coated-aggregate model, and there are leakage points in both models. In addition, we also compared the retrieval results of BC particles coated with OC and BrC, respectively, and the trend is consistent with the retrieval results of BC particles coated with sulfate. However, it is worth noting that there are more leakage points in the retrieval results of the mixing state of BC particles coated with BrC, which indicates that SP2 will lose a lot of data in the retrieval of the mixing state of BC particles coated with BrC.

Figure 1. Retrieval results of mixing state of sulfate-coated BC particles with different fractal dimensions. (a, b) lightly coated BC particles with volume equivalent particle size ratios of 2.71 and 2.37, respectively. (c, d) heavily coated BC particles with volume equivalent particle size ratios of 2.71 and 2.37, respectively.

Figure 2 shows the retrieval results of the closed-cell model mixing states of BC particles coated by different coating materials. The retrieval results of the mixing state of BC particles coated by sulfate and OC are similar, and the points and lines in the figure are basically identical. This is because the complex refractive indices of sulfate and OC at 1064nm wavelength are very similar, resulting in analogical optical properties calculation results, and thus similar retrieval results of their mixing states. However, the retrieval results of the mixing state of BC particles coated with BrC are obviously different from those of BC particles coated with sulfate and OC. The difference increases with the increase of fractal dimension, but the volume equivalent particle size ratio has little effect on it. For the light-coated BC particles with fractal dimensions 1.80 and 2.40, the retrieval results of the mixing state of the BC particles coated with BrC are slightly smaller than the retrieval results of the mixing state of the black carbon particles coated with sulfate and OC. The retrieval error of the mixing state of the BC particles coated by BrC with larger fractal dimension is smaller than that of the BC particles coated by sulfate and OC, indicating that SP2 can measure the mixing state of the BC particles lightly coated by BrC with larger fractal dimension more accurately.

Figure 2. Retrieval results of closed-cell model mixing states of BC particles coated with different materials.

Figure. 3 shows the retrieval results of the mixing state of the coated BC particles coated with different materials by the coated-aggregate model. There are also leakage points in the retrieval results of heavily coated BC particles with different coating materials, but the overall trend is clear and consistent under different fractal dimensions. With the increase of particle size, the D_p/D_c retrieval results gradually converge to 1. Different from the light-coated BC particles, the retrieval results of the mixing state of the heavily-coated BC particles coated with sulfate and OC no longer coincide, but show a slight difference. The retrieval results of the mixing state of BC particles heavily coated with BrC are significantly different from those of BC particles heavily coated with sulfate and OC. They are similar to the retrieval results of the closed-cell model with a large fractal dimension (D_f=2.60) shown in Fig 2. These results are higher than the retrieval results of the mixing state of BC particles heavily coated with sulfate and OC. This also illustrates that SP2 can measure the mixing state of BC

https://doi.org/10.5194/egusphere-2024-3781
Preprint. Discussion started: 21 January 2025

particles heavily coated with BrC with higher accuracy. In addition, the difference between the retrieval results of the mixing state of BC particles heavily coated with BrC and that of BC particles heavily coated with sulfate and OC increases with the increase of fractal dimension and decreases with the increase of volume equivalent particle size ratio. The maximum retrieval error of the mixing state of the BC particles heavily coated with three different materials is -63.1%, which appears on the BC particles heavily coated with sulfate and OC with a fractal dimension of 2.60.

Figure 3. Retrieval results of the coated-aggregate model mixing states of BC particles coated with different materials.

3.2 Effect of coatings materials on the retrieval of the mixing state of BC particle groups

Figure 4. Distribution of retrieval results for black carbon particles coated with different materials. The light-colored part on the left of the half-violin diagram is the retrieval result distribution of the closed-cell model, and the dark-colored part on the right is the retrieval result distribution of the coated-aggregate model.

First, in order to understand the distribution of BC particles over the entire size range, we drew a half-violin diagram as shown in **Figure 4**. The dashed lines in the figure represent the average of the retrieval results, and the fractal dimension of all models is 2.60. Like the violin plot, the width of the half-side filled in the half-violin plot also represents the probability distribution of the retrieval result. Three distinct regions, purple, yellow, and red, represent the distribution of retrieval results for black carbon particles coated with sulfate, OC, and BrC, respectively. It can be seen from the figure that the distribution of retrieval results for BC particles coated with sulfate and OC is basically the same, and the average retrieval results of different models increase with the increase of the preset volume equivalent particle size ratio. The average value of the lightly coated BC particles represented by the closed-cell model is smaller than that of the heavily coated black carbon particles represented by the coated-aggregate model under the same volume equivalent particle size ratio. The retrieval result distribution of BC particles coated with BrC is obviously different from that of BC particles coated with the other two materials, and the probability distribution width is significantly smaller than that of the other two materials. This is because the retrieval result of BC particles coated with BrC has significantly more leakage points than the other two materials, resulting in a small amount of data. This can also be seen from the retrieval results of the fractal dimension of 2.60 corresponding to **Figures 2 and 3**. In addition, the average retrieval results of the BC particles lightly coated with BrC increase with the increase of the preset volume equivalent particle size ratio, but the average retrieval results of the heavily coated BC particles decrease with the increase of the preset volume equivalent particle size ratio, which makes the retrieval error larger.

Because the aerosol in the real atmosphere does not exist as a single particle, it is more meaningful to study the mixing state of the BC aerosol population for practical application. Therefore, under the assumption that the equivalent volume diameter of BC particles follows the lognormal distribution law, we consider the retrieval results of the mixing state of BC particles with different coating materials. The retrieval results and relative errors of the mixing state of BC particles coated with different coating materials are shown in **Table 1**. For the light-coated black carbon particles represented by the closed-cell model, the mixing state retrieval results and relative errors of BC particles with different coating materials are not very different, and the relative errors decrease with the reduction of fractal dimension and volume-equivalent particle size ratio. However, for the heavily coated black carbon particles represented by the coated-aggregate model, the mixing state retrieval results and relative errors of the BC particles coated with BrC are significantly different from those of the BC particles coated with the other two materials. The relative error of black carbon particle swarm retrieval results heavily coated with sulfate and OC is smaller than that for BC particles lightly coated with these two materials. It is worth noting that the relative error of the retrieval results of the mixing state of black carbon particles heavily coated with BrC fluctuates positively and negatively, which is caused by too many leakage points in the retrieval results of heavily coated BC particles under this coating material. This shows that the missing points when SP2 is used to measure the mixing state of BC particles heavily coated with BrC will have a great influence on the retrieval results of the mixing state of the particle swarm.

Table 1. Retrieval results and relative error of mixing state of black carbon particles with different coating materials.

3.3 Impact of SP2 retrieval errors on BC absorption enhancement estimates

After BC particles undergo the aging process in the atmosphere, the influence of non-BC materials coated in BC nuclei on the light absorption capacity of BC particles is often called the "prism effect"(Cui et al., 2016), which can increase the absorption cross-section of BC particles. Previous studies have applied the retrieval results of SP2 to calculate the mass absorption cross section (MAC) of coated BC particles to obtain the enhanced absorption of coated BC particles (Eab)(Zhang et al., 2023). However, considering that there are errors in SP2 retrieval of the mixing state of BC particles, there are also errors in the estimation of absorption enhancement. Therefore, this section analyzes the effect of SP2 retrieval error on the estimation of enhanced absorption of BC coated by different materials from the perspective of numerical simulation.

Figure 5. shows the absorption enhancement of the closed-cell model and the core-shell model coated by different coating materials. The solid point line is the actual value (AV) of the absorption enhancement of light-coated BC particles represented by the closed-cell model, while the hollow point line is the absorption enhancement of coated BC particles derived from the retrieval results of the core-shell model. It can be seen from the figure that the absorption enhancement values of the BC particles coated with three different materials derived from the SP2 retrieval value (RV) basically overlap, and the trend is consistent under different volume equivalent particle size ratios, but it decreases with the increase of the diameter of the BC core, and the value ranges from 1.0 to 3.16. The diameter of the BC core has little effect on the absorption enhancement of the actual coated BC particles, but the materials of the coated BC have a certain effect. The

https://doi.org/10.5194/egusphere-2024-3781
Preprint. Discussion started: 21 January 2025

actual absorption enhancement values of the BC particles coated with sulfate and OC are similar, and the values are basically stable between 1.0 and 2.0 under different volume-equivalent particle size ratios and BC core diameters. However, the BC particles coated with BrC are significantly different from the BC particles coated with these two materials, and the difference decreases with the decrease of volume equivalent particle size ratio. That is, the absorption enhancement of the actual BC particles coated with BrC decreases with the decrease of the volume equivalent particle size ratio. In addition, the relative errors between the BC absorption enhancement retrieval values and the actual values of the three coating materials under all parameters of the closed-cell model are calculated. The results show that the relative error of absorption enhancement of BC particles coated with BrC is negative in most cases, and the minimum can reach -83.9%, which indicates that the retrieval value of SP2 underestimates its absorption enhancement. However, for most BC particles coated with sulfate and OC, the retrieval value of SP2 overestimates their absorption enhancement.

Figure 5. Enhanced absorption of BC particles lightly coated with different materials. (a-d) the closed-cell model with fractal dimensions of 1.80, and the volume equivalent particle size ratios are 2.71, 2.37, 2.15, and 1.36, respectively. The solid point plot is the actual value of the absorption enhancement of the coated BC particles, and the hollow point plot is the absorption enhancement of the coated BC particles derived from the SP2 retrieval results.

Figure 6. The absorption of BC particles heavily coated with different materials is enhanced, and the legend is the same as in Fig 4. The first column is the coated-aggregate model with a fractal dimension of 2.60 and the volume equivalent particle size of 2.71, 2.37, and 2.15, respectively. The second column is a coated-aggregate model with a fractal dimension of 2.80 and the remaining parameters are the same as those of the first column.

Figure 6. shows the absorption enhancement of the coated-aggregate model and core-shell model coated with different materials. The solid and hollow dots represent the same values as in **Figure 5**. There are obvious differences in the absorption enhancement values of BC particles coated by three different materials based on SP2 retrieval values. Under the same morphological parameters, the absorption enhancement of BrC-coated BC particles is the strongest, followed by that coated with OC and that coated with sulfate. The actual value of enhanced absorption of BC particles coated with BrC is significantly different from that of BC particles coated with sulfate and OC, and the actual value of enhanced absorption of BC particles coated with BrC is always the largest, which also indicates that the measurement error of SP2 has the greatest impact on the estimation of enhanced absorption of BC heavily coated with BrC. In most cases, the relative error between the actual value and the retrieval value of the absorption enhancement of the BC particles coated by three different materials is negative, which indicates that the retrieval value of SP2 underestimates its absorption enhancement. The relative error of

https://doi.org/10.5194/egusphere-2024-3781
Preprint. Discussion started: 21 January 2025

absorption enhancement of BC particles heavily coated with BrC is as low as -77.6%. The relative error of absorption enhancement of BC particles heavily coated with sulfate and OC is -61.9%. For both the coated-aggregate model and the closed-cell model, the absorption enhancement error of the BC particles coated with BrC is greater than that of the BC particles coated with sulfate and OC, indicating that the accuracy of calculating the absorption enhancement of the BC particles coated with BrC is the lowest according to the retrieval results of SP2.

3.4 Effects of SP2 retrieval errors on the calculation of BC radiative forcing using simple forcing efficiency equation

The measurement error of the mixing state of BC aerosols will affect the input of the radiative transfer mode, and thus affect the estimation of the radiative effect of BC aerosols. The simple forcing efficiency equation focuses on describing the forcing effect of particles with different particle sizes in a certain wavelength range, reflecting the influence of uniform thin aerosols in the lower atmosphere on radiative forcing (Peng et al., 2022). In this section, a simple forcing efficiency equation is used to quantify the radiative forcing estimation error caused by SP2 retrieval of mixing state errors of BC particles with different coating materials at 1064 nm.

Table 2. shows the actual and SP2 retrieval values and corresponding retrieval errors of the simple forcing efficiency of BC particles coated with BrC, sulfate, and OC. As there are too many leakage points in the retrieval result of the coated-aggregate model, it will not be discussed here. The "actual value (AV) " in the table is the simple forcing efficiency of actual light-coated and heavy-coated BC particles with different coating materials expressed by a closed-cell model, whose optical properties are obtained using MSTM. The " retrieval value (RV) " is the optical equivalent core-shell model based on SP2 retrieval results, and the simple forcing efficiency obtained from the mass scattering cross section and mass absorption cross section calculated using Mie scattering theory. For BC particles with different coating materials, the actual and retrieval values are similar even if the fractal dimensions are different for the same volume equivalent particle size ratio. It can be seen that the fractal shape of the model has little effect on the radiative forcing estimation. However, the retrieval error range of the simple radiative forcing efficiency of BC particles with different coating materials is different. The retrieval error of the simple radiative forcing efficiency of BC particles coated with BrC is greater than that of BC particles coated with the other two materials, ranging from -89.9% to -80.5%. The retrieval error of the simple radiative forcing efficiency of BC particles coated with sulfate and OC is similar, ranging from -64.3% to -38.4%.

Table 2. The actual and SP2 retrieval values of the simple forcing efficiency of BC particles coated with BrC, sulfate, and OC

4. Conclusions

In this paper, the mixing state of black carbon particles with three different coating materials of sulfate, BrC, and OC was retrieved to explore the accuracy of SP2 in measuring the mixing state of black carbon particles. The effects of the error of SP2 retrieval of mixing state of black carbon particles on the estimation of absorption enhancement and radiative forcing of black carbon particles with different coating materials are analyzed. The main conclusions are summarized as follows:

(1) The retrieval results of the single particle mixing state of BC particles coated with sulfate and OC are similar. The retrieval results of the mixing state of the black carbon particles coated with BrC are greater than those of the black carbon particles coated with the other two materials under different coating structures. This indicates that the relative error of SP2 in retrieving the mixing state of BrC-coated BC particles is small. However, SP2 missed more data when retrieving the mixing state of black carbon particles coated with BrC than the other two materials.

(2) For the light-coated black carbon particles represented by the closed-cell model, the mixing state retrieval results and relative errors of the black carbon particle swarm with different coating materials following a certain lognormal distribution have little difference. However, due to the omission of the retrieval results, for the heavily coated black carbon particles represented by the coated-aggregate model, the retrieval results and relative errors of the mixing state of the black carbon particles coated with BrC are significantly different from those of the black carbon particles coated with the other two materials. The relative error fluctuated positively and negatively.

(3) The effect of mixing state retrieval error on absorption enhancement (E_{ab}) of coated black carbon particles is calculated by using SP2 retrieval results. The absorption enhancement error of black carbon particles coated with BrC is greater than that of black carbon particles coated with sulfate and OC, indicating that the accuracy of calculating the absorption enhancement of black carbon particles coated with BrC based on SP2 retrieval results is the lowest.

(4) At 1064 nm, the retrieval error of the simple radiative forcing efficiency of the black carbon particles coated with BrC is larger than that of the black carbon particles coated with the other two materials, with the highest error reaching -89.9%. The retrieval error of the simple radiative forcing efficiency of black carbon particles coated with sulfate and OC is similar, ranging from -64.3% to -38.4%.

Data availability. The data for this study is available online (https://doi.org/10.13140/RG.2.2.22582.72008).

Author contributions. JL: conceptualization, methodology, funding acquisition, and co-writing of the original draft; DZ: methodology, experiment, formal analysis, and co-writing of the original draft; GW: experiment, data curation, and manuscript review and editing; CZ: formal analysis, data curation, and manuscript review and editing; and XZ: data curation as well as manuscript review and editing.

https://doi.org/10.5194/egusphere-2024-3781
Preprint. Discussion started: 21 January 2025

Competing interests. The contact author has declared that none of the authors has any competing interests.

Acknowledgments. We particularly thank Dr. Mishchenko M. I. and Dr. Mackowski D. W. for the MSTM code.

Financial support. This research has been supported by the National Natural Science Foundation of China (grant no. 42305082), the China Postdoctoral Science Foundation (grant no. 2024M750493), and the China Meteorological Administration Xiong'an Atmospheric Boundary Layer Key Laboratory (grant no. 2023LABL-B15).

References

Adachi, K., Zaizen, Y., Kajino, M., and Igarashi, Y.: Mixing state of regionally transported soot particles and the coating effect on their size and shape at a mountain site in Japan, Journal of Geophysical Research-Atmospheres, 119, 5386-5396, 10.1002/2013jd020880, 2014.

Bond, T. C. and Bergstrom, R. W.: Light absorption by carbonaceous particles: An investigative review, Aerosol Sci. Technol., 40, 27-67, 10.1080/02786820500421521, 2006.

Bond, T. C., Doherty, S. J., Fahey, D. W., Forster, P. M., Berntsen, T., DeAngelo, B. J., Flanner, M. G., Ghan, S., Kärcher, B., Koch, D., Kinne, S., Kondo, Y., Quinn, P. K., Sarofim, M. C., Schultz, M. G., Schulz, M., Venkataraman, C., Zhang, H., Zhang, S., Bellouin, N., Guttikunda, S. K., Hopke, P. K., Jacobson, M. Z., Kaiser, J. W., Klimont, Z., Lohmann, U., Schwarz, J. P., Shindell, D., Storelvmo, T., Warren, S. G., and Zender, C. S.: Bounding the role of black carbon in the climate system: A scientific assessment, J. Geophys. Res.-Atmos., 118, 5380-5552, 10.1002/jgrd.50171, 2013.

Ceolato, R., Paulien, L., Maughan, J. B., Sorensen, C. M., and Berg, M. J.: Radiative properties of soot fractal superaggregates including backscattering and depolarization, Journal of Quantitative Spectroscopy & Radiative Transfer, 247, 8, 10.1016/j.jqsrt.2020.106940, 2020.

China, S., Mazzoleni, C., Gorkowski, K., Aiken, A. C., and Dubey, M. K.: Morphology and mixing state of individual freshly emitted wildfire carbonaceous particles, Nature Communications, 4, 7, 10.1038/ncomms3122, 2013.

Cui, X., Wang, X., Yang, L., Chen, B., Chen, J., Andersson, A., and Gustafsson, Ö.: Radiative absorption enhancement from coatings on black carbon aerosols, Sci. Total Environ., 551, 51-56, 2016.

Ding, A. J., Huang, X., Nie, W., Sun, J. N., Kerminen, V. M., Petäjä, T., Su, H., Cheng, Y. F., Yang, X. Q., Wang, M. H., Chi, X. G., Wang, J. P., Virkkula, A., Guo, W. D., Yuan, J., Wang, S. Y., Zhang, R. J., Wu, Y. F., Song, Y., Zhu, T., Zilitinkevich, S., Kulmala, M., and Fu, C. B.: Enhanced haze pollution by black carbon in megacities in China, Geophysical Research Letters, 43, 2873-2879, 10.1002/2016gl067745, 2016.

Gao, R. S., Schwarz, J. P., Kelly, K. K., Fahey, D. W., Watts, L. A., Thompson, T. L., Spackman, J. R., Slowik, J. G., Cross, E. S., Han, J. H., Davidovits, P., Onasch, T. B., and Worsnop, D. R.: A novel method for estimating light-scattering properties of soot aerosols using a modified single-particle soot photometer, Aerosol Sci. Technol., 41, 125-135, 10.1080/02786820601118398, 2007.

Kahnert, M. and Kanngiesser, F.: Modelling optical properties of atmospheric black carbon aerosols, J. Quant. Spectrosc. Radiat. Transf., 244, 17, 10.1016/j.jqsrt.2020.106849, 2020.

Kholghy, M., Saffaripour, M., Yip, C., and Thomson, M. J.: The evolution of soot morphology in a laminar coflow diffusion flame of a surrogate for Jet A-1, Combust. Flame, 160, 2119-2130, 10.1016/j.combustflame.2013.04.008, 2013.

Lei, Y. D., Zhang, F., Miao, L. J., Yu, Q. R., Duan, M. K., Fraedrich, K., and Yu, Z. F.: Potential impacts of future reduced aerosols on internal dynamics characteristics of precipitation based on model simulations over southern China, Physica A, 545, 13, 10.1016/j.physa.2019.123808, 2020.

Li, F., Luo, B., Zhai, M. M., Liu, L., Zhao, G., Xu, H. B., Deng, T., Deng, X. J., Tan, H. B., Kuang, Y., and Zhao, J.: Black carbon content of traffic emissions significantly impacts black carbon mass size distributions and mixing states, Atmos. Chem. Phys., 23, 6545-6558, 10.5194/acp-23-6545-2023, 2023.

Li, J., Posfai, M., Hobbs, P. V., and Buseck, P. R.: Individual aerosol particles from biomass burning in southern Africa: 2, Compositions and aging of inorganic particles, J. Geophys. Res.-Atmos., 108, 12, 10.1029/2002jd002310, 2003.

Li, Y., Kang, S. C., Chen, J. Z., Hu, Z. F., Wang, K., Paudyal, R., Liu, J. S., Wang, X. X., Qin, X., and Sillanpää, M.: Black carbon in a glacier and snow cover on the northeastern Tibetan Plateau: Concentrations, radiative forcing and potential source from local topsoil, Sci. Total Environ., 686, 1030-1038, 10.1016/j.scitotenv.2019.05.469, 2019.

Liu, D., Allan, J. D., Young, D. E., Coe, H., Beddows, D., Fleming, Z. L., Flynn, M. J., Gallagher, M. W., Harrison, R. M., Lee, J., Prevot, A. S. H., Taylor, J. W., Yin, J., Williams, P. I., and Zotter, P.: Size distribution, mixing state and source apportionment of black carbon aerosol in London during wintertime, Atmos. Chem. Phys., 14, 10061-10084, 10.5194/acp-14-10061-2014, 2014.

Liu, H., Pan, X. L., Liu, D. T., Liu, X. Y., Chen, X. S., Tian, Y., Sun, Y. L., Fu, P. Q., and Wang, Z. F.: Mixing characteristics of refractory black carbon aerosols at an urban site in Beijing, Atmospheric Chemistry and Physics, 20, 5771-5785, 10.5194/acp-20-5771-2020, 2020.

Liu, H., Pan, X., Wang, D., Liu, X., Tian, Y., Yao, W., Lei, S., Zhang, Y., Li, J., Lei, L., Xie, C., Fu, P., Sun, Y., and Wang, Z.: Mixing characteristics of black carbon aerosols in a coastal city using the CPMA-SP2 system, Atmospheric Research, 265, 10.1016/j.atmosres.2021.105867, 2022.

Liu, J., Wang, L., Wang, G. Y., and Zhang, X. H.: Numerical investigation on the accuracy of size information of fractal soot aerosols retrieved by lidar: Optical property, morphology effect, and parameterization scheme, J. Quant. Spectrosc. Radiat. Transf., 295, 12, 10.1016/j.jqsrt.2022.108435, 2023a.

https://doi.org/10.5194/egusphere-2024-3781
Preprint. Discussion started: 21 January 2025

Liu, J., Wang, G., Zhu, C., Zhou, D., and Wang, L.: Numerical investigation on retrieval errors of mixing states of fractal black carbon aerosols using single-particle soot photometer based on Mie scattering and the effects on radiative forcing estimation, Atmos. Meas. Tech., 16, 4961-4974, 10.5194/amt-16-4961-2023, 2023b.

Liu, J., Wang, G. Y., Zhu, C. C., Zhou, D. H., and Wang, L.: Numerical investigation on retrieval errors of mixing states of fractal black carbon aerosols using single-particle soot photometer based on Mie scattering and the effects on radiative forcing estimation, Atmos. Meas. Tech., 16, 4961-4974, 10.5194/amt-16-4961-2023, 2023c.

Luo, J., Zhang, Y. M., and Zhang, Q. X.: Effects of black carbon morphology on brown carbon absorption estimation: from numerical aspects, Geosci. Model Dev., 14, 2113-2126, 10.5194/gmd-14-2113-2021, 2021.

Murphy, D. M., Froyd, K. D., Schwarz, J. P., and Wilson, J. C.: Observations of the chemical composition of stratospheric aerosol particles, Q. J. R. Meteorol. Soc., 140, 1269-1278, 10.1002/qj.2213, 2014.

Peng, H. Y., Wang, Y. S., Wang, Y. L., Chen, Y. K., Li, D., and Xue, H.: Characteristics of emission and light-absorption of size-segregated carbonaceous aerosol emitted from four types of coal combustion at different combustion temperatures, Atmos. Pollut. Res., 13, 10, 10.1016/j.apr.2021.101265, 2022.

Santoso, M., Lestiani, D. D., Kurniawati, S., Damastuti, E., Kusmartini, I., Atmodjo, D. P. D., Sari, D. K., Hopke, P. K., Mukhtar, R., Muhtarom, T., Tjahyadi, A., Parian, S., Kholik, N., Sutrisno, D. A., Wahyudi, D., Sitorus, T. D., Djamilus, J., Riadi, A., Supriyanto, J., Dahyar, N., Sondakh, S., Hogendorp, K., Wahyuni, N., Bejawan, I. G., and Suprayadi, L. S.: Assessment of Urban Air Quality in Indonesia, Aerosol Air Qual. Res., 20, 2142-2158, 10.4209/aaqr.2019.09.0451, 2020.

Schwarz, J. P., Gao, R. S., Fahey, D. W., Thomson, D. S., Watts, L. A., Wilson, J. C., Reeves, J. M., Darbeheshti, M., Baumgardner, D. G., Kok, G. L., Chung, S. H., Schulz, M., Hendricks, J., Lauer, A., Kärcher, B., Slowik, J. G., Rosenlof, K. H., Thompson, T. L., Langford, A. O., Loewenstein, M., and Aikin, K. C.: Single-particle measurements of midlatitude black carbon and light-scattering aerosols from the boundary layer to the lower stratosphere, J. Geophys. Res.-Atmos., 111, 15, 10.1029/2006jd007076, 2006.

Sorensen and Roberts: The Prefactor of Fractal Aggregates, Journal of colloid and interface science, 186, 447-452, 10.1006/jcis.1996.4664, 1997.

Wang, S. R., Zhou, K. L., Lu, X. H., Chen, H., Yang, F., Li, Q., Yang, X., and Wang, X. F.: Measurement of Density and Shape for Single Black Carbon Aerosols in a Heavily Polluted Urban Area, Aerosol Air Qual. Res., 21, 16, 10.4209/aaqr.210162, 2021.

Wang, Y. Q., Zhang, X. Y., Sun, J. Y., Zhang, X. C., Che, H. Z., and Li, Y.: Spatial and temporal variations of the concentrations of PM₁₀, PM_{2.5} and PM₁ in China, Atmospheric Chemistry and Physics, 15, 13585-13598, 10.5194/acp-15-13585-2015, 2015.

Wang, Y. Y., Liu, F. S., He, C. L., Bi, L., Cheng, T. H., Wang, Z. L., Zhang, H., Zhang, X. Y., Shi, Z. B., and Li, W. J.: Fractal Dimensions and Mixing Structures of Soot Particles during Atmospheric Processing, Environ. Sci. Technol. Lett., 4, 487-493, 10.1021/acs.estlett.7b00418, 2017.

Wozniak, M., Onofri, F. R. A., Barbosa, S., Yon, J., and Mroczka, J.: Comparison of methods to derive morphological parameters of multi-fractal samples of particle aggregates from TEM images, J. Aerosol. Sci., 47, 12-26, 10.1016/j.jaerosci.2011.12.008, 2012.

Zeng, C., Liu, C., Li, J. N., Zhu, B., Yin, Y., and Wang, Y.: Optical Properties and Radiative Forcing of Aged BC due to Hygroscopic Growth: Effects of the Aggregate Structure, J. Geophys. Res.-Atmos., 124, 4620-4633, 10.1029/2018jd029809, 2019.

Zhang, J., Wang, Y. Y., Teng, X. M., Liu, L., Xu, Y. S., Ren, L. H., Shi, Z. B., Zhang, Y., Jiang, J. K., Liu, D. T., Hu, M., Shao, L. Y., Chen, J. M., Martin, S. T., Zhang, X. Y., and Li, W. J.: Liquid-liquid phase separation reduces radiative absorption by aged black carbon aerosols, Communications Earth & Environment, 3, 9, 10.1038/s43247-022-00462-1, 2022.

Zhang, X. L., Wang, Y. Z., Zhou, Y., Wang, J. Y., and Mao, M.: Significance of Absorbing Fraction of Coating on Absorption Enhancement of Partially Coated Black Carbon Aerosols, Atmosphere, 12, 13, 10.3390/atmos12111422, 2021.

Zhang, Y. T., Liu, H., Lei, S. D., Du, A. D., Yao, W. J., Tian, Y., Sun, Y. L., Xin, J. Y., Li, J., Cao, J. J., Wang, Z. F., and Pan, X. L.: Size-resolved mixing state of ambient refractory black carbon aerosols in Beijing during the XXIV Olympic winter games, Atmos. Environ., 301, 13, 10.1016/j.atmosenv.2023.119672, 2023.

Zhang, Y. X., Zhang, Q., Yao, Z. L., and Li, H. Y.: Particle Size and Mixing State of Freshly Emitted Black Carbon from Different Combustion Sources in China, Environmental Science & Technology, 54, 7766-7774, 10.1021/acs.est.9b07373, 2020.

Zhang, Y. X., Li, M., Cheng, Y. F., Geng, G. N., Hong, C. P., Li, H. Y., Li, X., Tong, D., Wu, N. N., Zhang, X., Zheng, B., Zheng, Y. X., Bo, Y., Su, H., and Zhang, Q.: Modeling the aging process of black carbon during atmospheric transport using a new approach: a case study in Beijing, Atmos. Chem. Phys., 19, 9663-9680, 10.5194/acp-19-9663-2019, 2019.

https://doi.org/10.5194/egusphere-2024-3781
Preprint. Discussion started: 21 January 2025

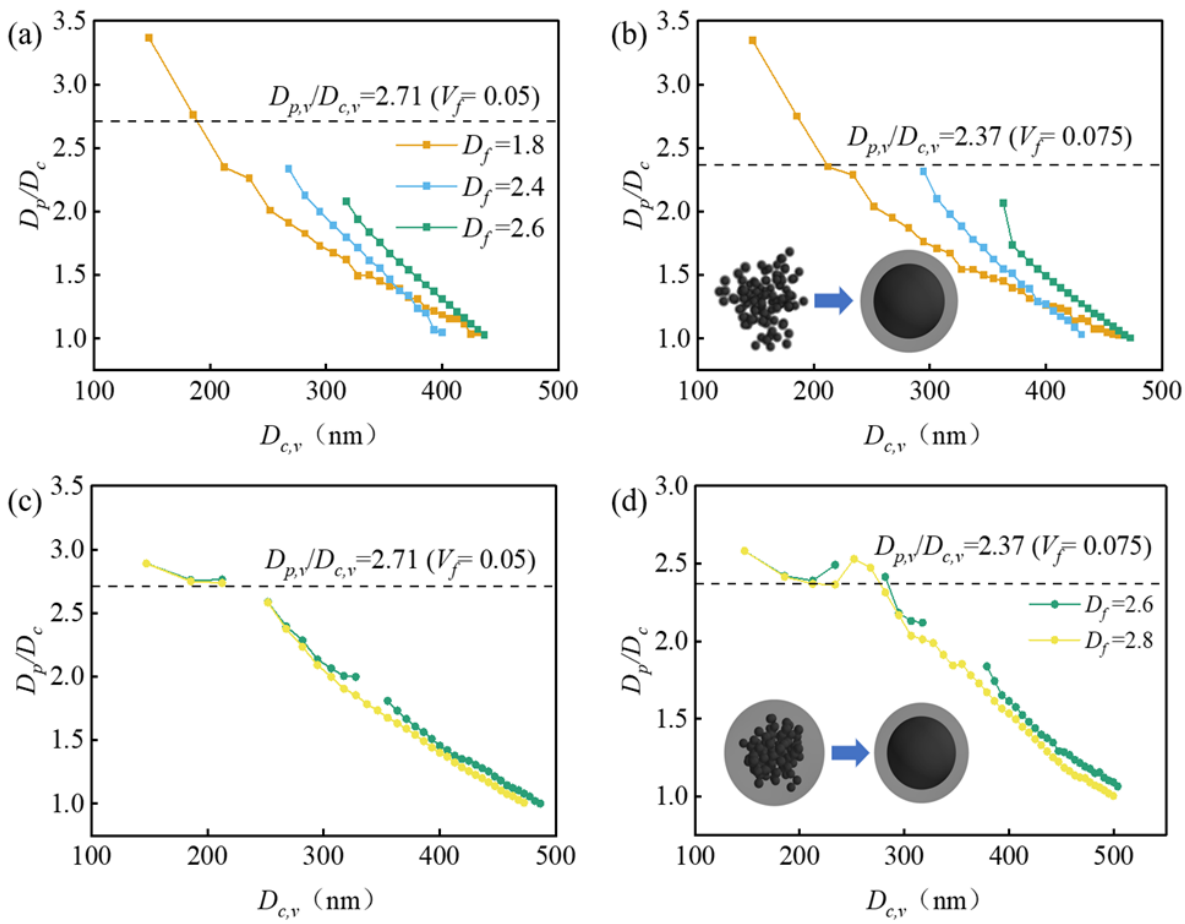

Figure 1. Retrieval results of mixing state of sulfate-coated BC particles with different fractal dimensions. (a, b) lightly coated BC particles with volume equivalent particle size ratios of 2.71 and 2.37, respectively. (c, d) heavily coated BC particles with volume equivalent particle size ratios of 2.71 and 2.37, respectively.

515

https://doi.org/10.5194/egusphere-2024-3781
Preprint. Discussion started: 21 January 2025

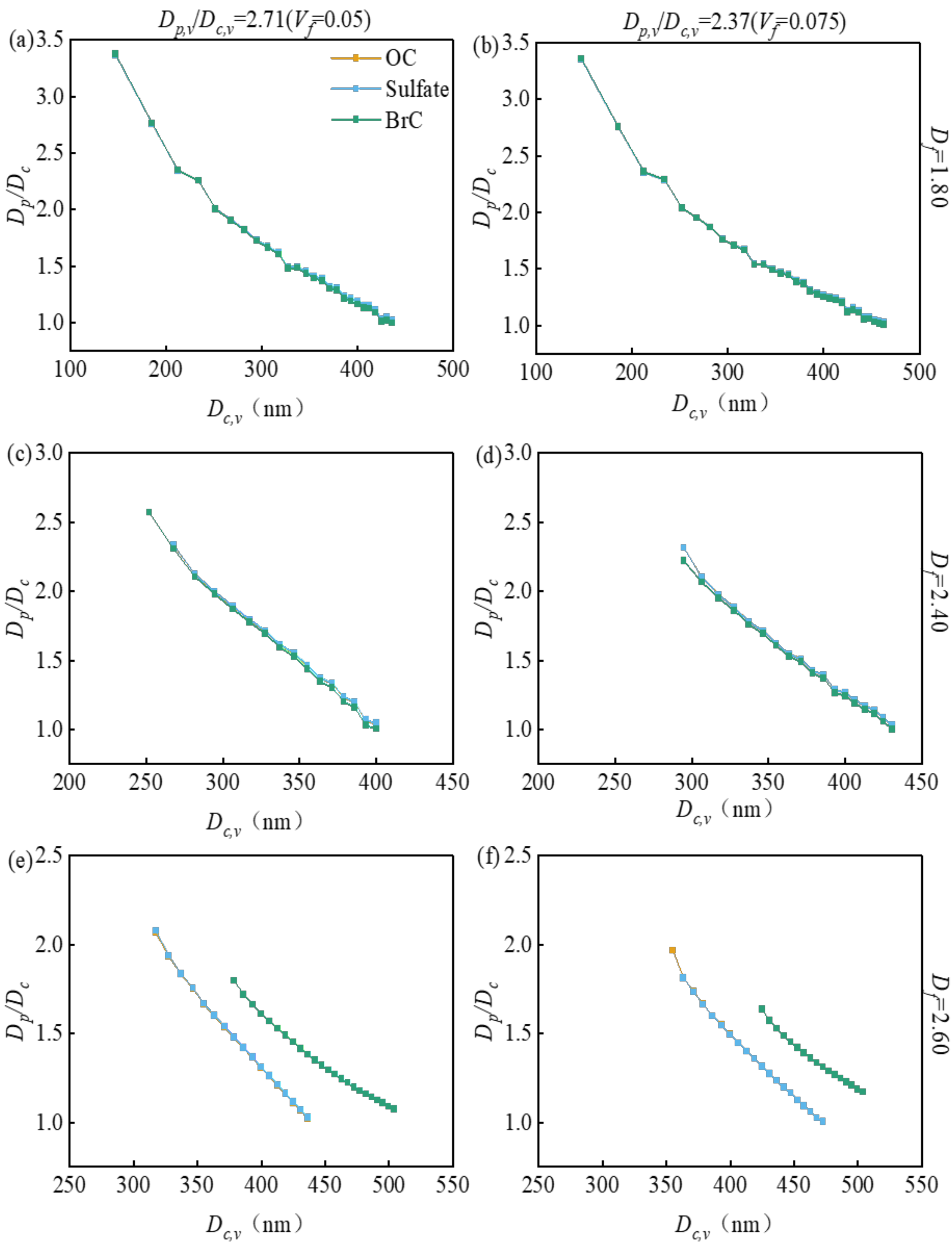

Figure 2. Retrieval results of closed-cell model mixing states of BC particles coated with different materials.

https://doi.org/10.5194/egusphere-2024-3781
Preprint. Discussion started: 21 January 2025

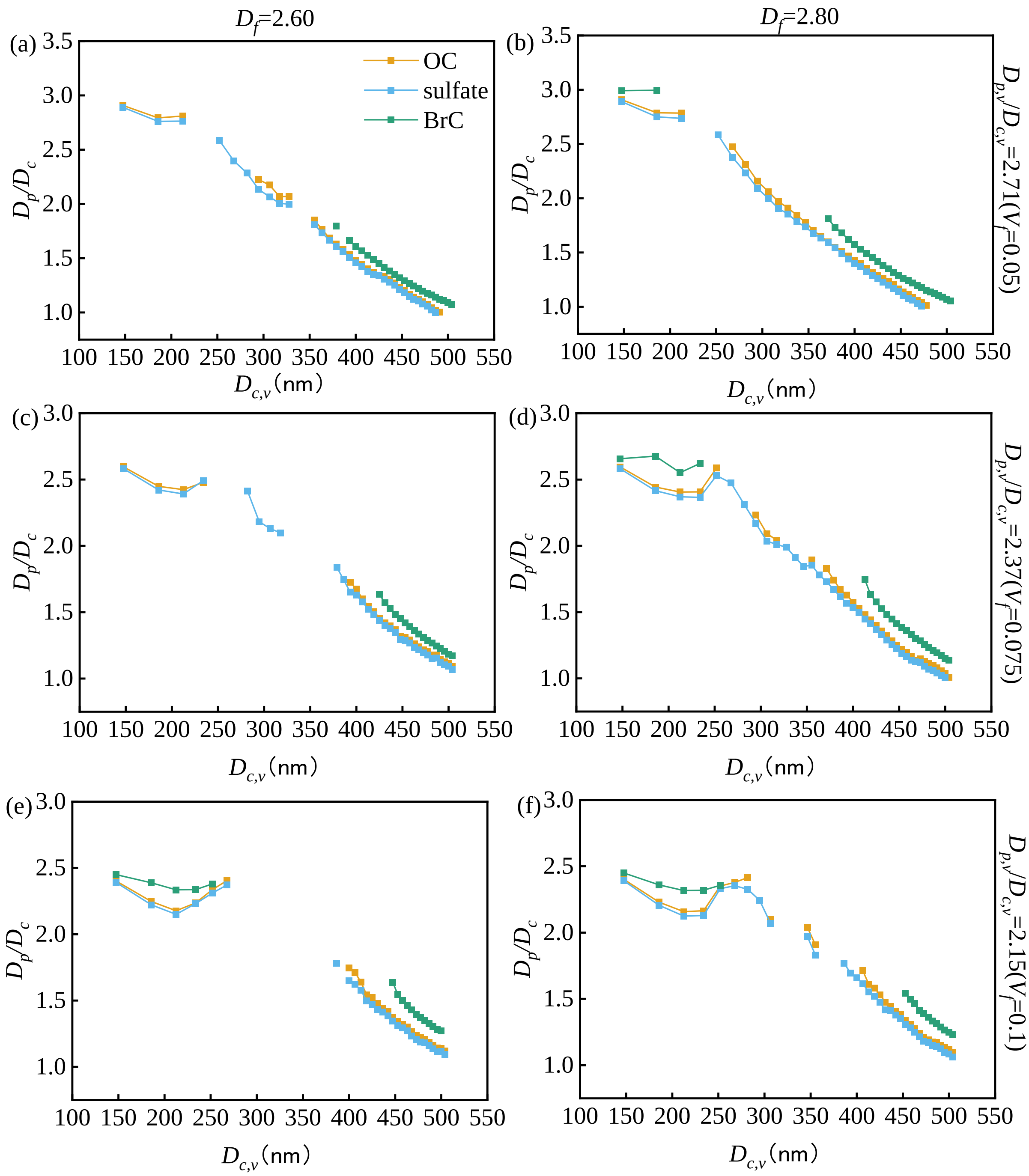

520 **Figure 3**. Retrieval results of the coated-aggregate model mixing states of BC particles coated with different materials.

https://doi.org/10.5194/egusphere-2024-3781
Preprint. Discussion started: 21 January 2025

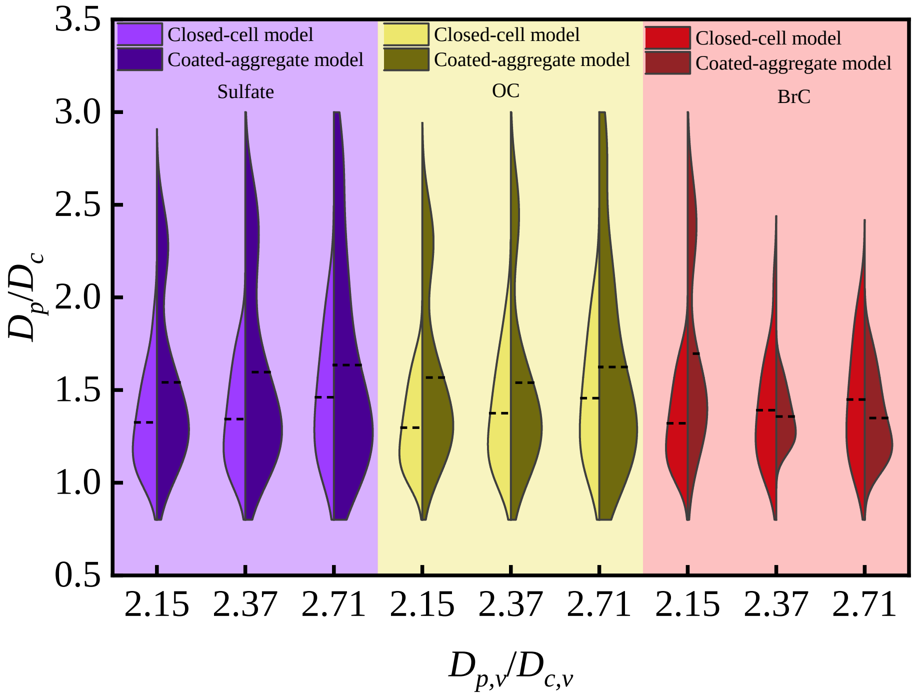

Figure 4. Distribution of retrieval results for black carbon particles coated with different materials. The light-colored part on the left of the half-violin diagram is the retrieval result distribution of the closed-cell model, and the dark-colored part on the right is the retrieval result distribution of the coated-aggregate model.

https://doi.org/10.5194/egusphere-2024-3781
Preprint. Discussion started: 21 January 2025

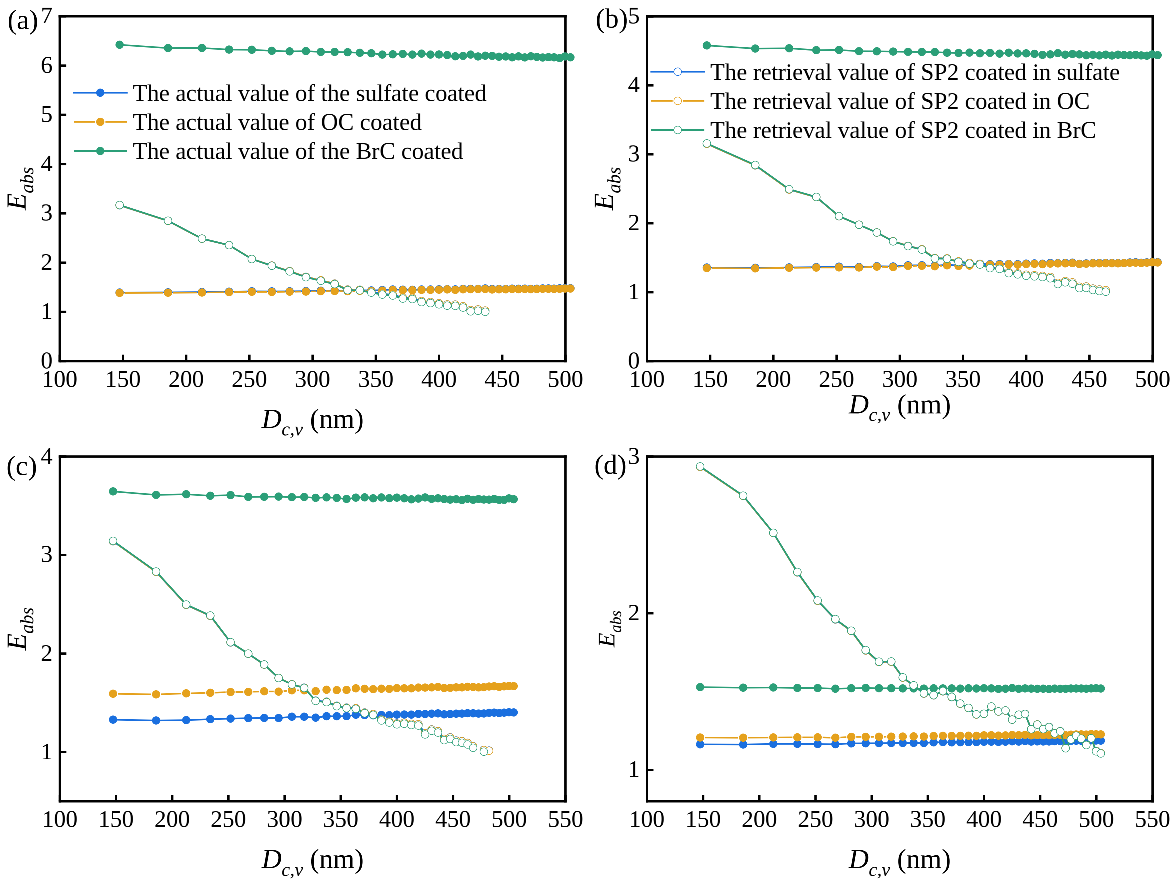

Figure 5. Enhanced absorption of BC particles lightly coated with different materials. (a-d) the closed-cell model with fractal dimensions of 1.80, and the volume equivalent particle size ratios are 2.71, 2.37, 2.15, and 1.36, respectively. The solid point plot is the actual value of the absorption enhancement of the coated BC particles, and the hollow point plot is the
530 absorption enhancement of the coated BC particles derived from the SP2 retrieval results.

https://doi.org/10.5194/egusphere-2024-3781
Preprint. Discussion started: 21 January 2025

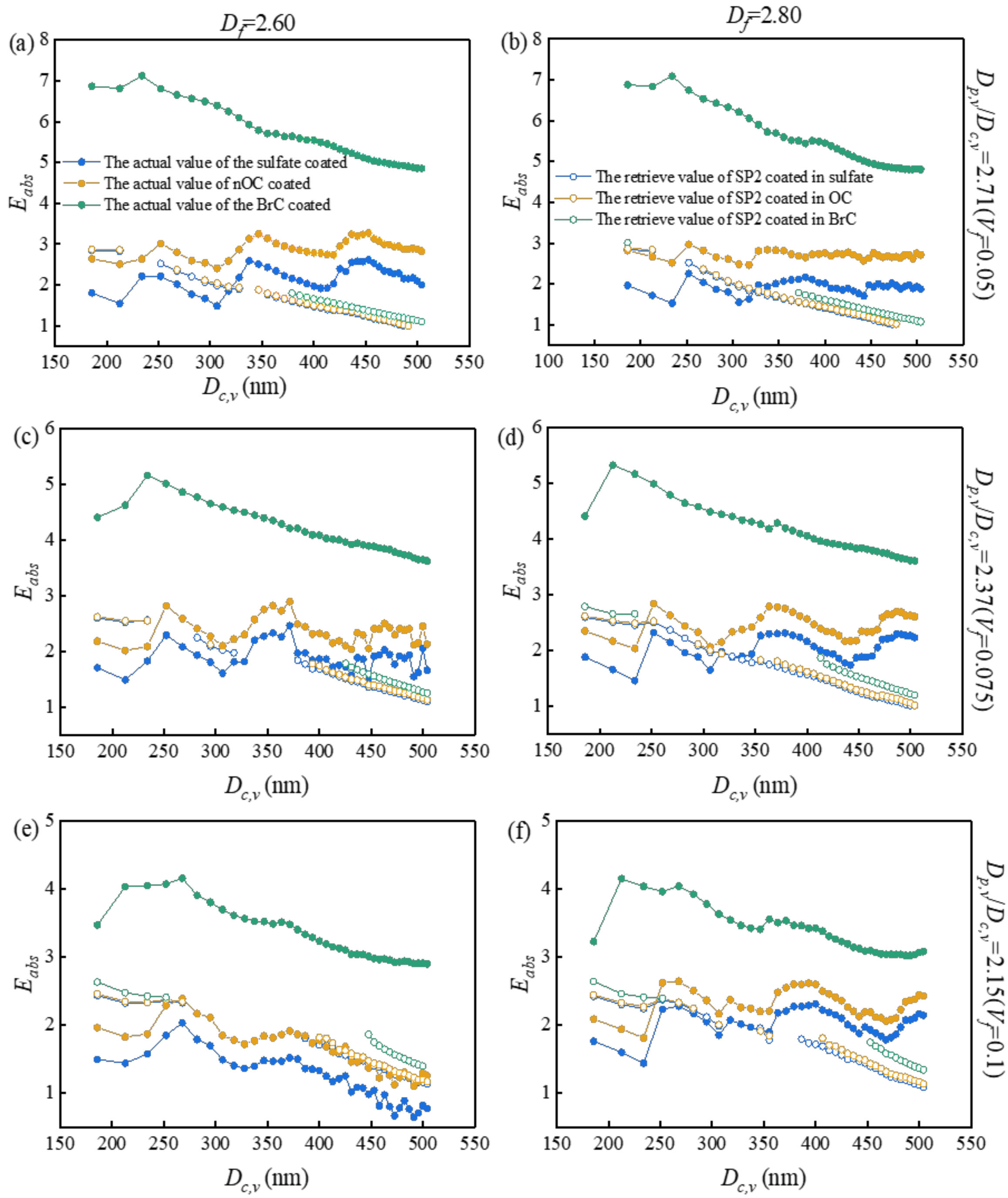

Figure 6. The absorption of BC particles heavily coated with different materials is enhanced, and the legend is the same as in Fig 4. The first column is the coated-aggregate model with a fractal dimension of 2.60 and the volume equivalent particle size of 2.71, 2.37, and 2.15, respectively. The second column is a coated-aggregate model with a fractal dimension of 2.80 and the remaining parameters are the same as those of the first column.

https://doi.org/10.5194/egusphere-2024-3781
Preprint. Discussion started: 21 January 2025

Table 1. Retrieval results and relative error of mixing state of black carbon particles with different coating materials.

Model		Closed-cell model						Coated-aggregate model			
D_f		1.80		2.40		2.60		2.60		2.8	
D_p/D_c	Coating material	RRs	RE	RRs	RE	RRs	RE	RRs	RE	RRs	RE
	BrC	1.45	-46.8%	1.27	-53.2%	1.26	-53.7%	1.26	-53.5	1.64	-39.6%
2.71	Sulfate	1.49	-45.2%	1.31	-51.8%	1.26	-53.6%	1.65	-39.2%	1.62	-40.3%
	OC	1.49	-45.2%	1.30	-52.0%	1.25	-53.9%	1.63	-40.0%	1.63	-40.1%
	BrC	1.47	-37.9%	1.25	-47.2%	1.23	-48.2%	1.31	-44.6%	2.09	-12.0%
2.37	Sulfate	1.51	-36.5%	1.28	-45.9%	1.20	-49.5%	1.91	-19.5%	1.75	-26.2%
	OC	1.51	-36.5%	1.28	-45.9%	1.20	-49.2%	1.96	-17.5%	1.78	-25.0%
	BrC	1.53	-29.0%	1.25	-42.1%	1.20	-44.1%	2.29	6.4%	2.27	5.2%
2.15	Sulfate	1.53	-28.9%	1.21	-43.8%	1.19	-44.9%	1.97	-8.7%	1.93	-10.2%
	OC	1.53	-29.1%	1.21	-43.9%	1.18	-45.2%	2.02	-6.2%	1.99	-7.4%

Table 2. The actual and SP2 retrieval values of the simple forcing efficiency of BC particles coated with BrC, sulfate, and OC

D_f		1.80			2.40			2.60		
D_p/D_c	Coating material	AV	RV	RRs	AV	RV	RRs	AV	RV	RRs
	BrC	0.71	0.08	-88.7%	0.71	0.09	-87.3%	0.71	0.08	-88.5%
2.71	Sulfate	0.15	0.08	-45.0%	0.16	0.10	-38.4%	0.16	0.08	-48.4%
	OC	0.15	0.08	-45.0%	0.22	0.09	-57.4%	0.23	0.08	-64.3%
	BrC	0.51	0.07	-85.6%	0.51	0.08	-84.2%	0.51	0.08	-85.2%
2.37	Sulfate	0.15	0.08	-49.1%	0.15	0.08	-44.4%	0.15	0.07	-54.0%
	OC	0.15	0.08	-49.2%	0.15	0.08	-44.3%	0.15	0.07	-53.3%
	BrC	0.40	0.07	-83.1%	0.40	0.08	-80.5%	0.41	0.07	-82.9%
2.15	Sulfate	0.15	0.07	-51.9%	0.15	0.08	-48.5%	0.15	0.07	-55.6%
	OC	0.18	0.07	-60.3%	0.18	0.08	-57.2%	0.15	0.07	-55.4%